HHS Public Access

Author manuscript

J Mol Cell Cardiol. Author manuscript; available in PMC 2025 September 15.

Published in final edited form as:

J Mol Cell Cardiol. 2025 April ; 201: 32–43. doi:10.1016/j.yjmcc.2025.01.011.

Mouse model of post-traumatic stress disorder negatively impacts cardiac homeostasis

Alexa Corker[a,b,c], **Miguel Troncoso**[c], **Maya Learmonth**[a,b], **Philip Broughton**[b], **Sara J. Sidles**[c,d], **Ryan Kelly**[c,d], **Shaoni Dasgupta**[a,b,c], **Thomas Dempster**[a,b,c], **Kim Vu**[a], **Amber Hazzard**[a,b,c], **An Van Laer**[b,c], **Rachel D. Penrod**[e], **Jeffery A. Jones**[a,c,f], **Amy D. Bradshaw**[a,b,c], **Michael R. Zile**[b,c], **Amanda C. LaRue**[c,d], **Kristine Y. DeLeon-Pennell**[a,b,c,*]

[a]College of Graduate Studies, Medical University of South Carolina, 171 Ashley Ave, Charleston, SC 29425, United States

[b]Department of Medicine, Division of Cardiology, Medical University of South Carolina, 171 Ashley Ave, Charleston, SC 29425, United States

[c]RResearch Service, Ralph H. Johnson Veterans Affairs Health Care System, 109 Bee St, Charleston, SC 29401, United States

[d]Department of Pathology & Laboratory Medicine, Medical University of South Carolina, 171 Ashley Ave, Charleston, SC 29425, United States

[e]Department of Neuroscience, Medical University of South Carolina, 171 Ashley Ave, Charleston, SC 29425, United States

[f]Department of Surgery, Medical University of South Carolina, 171 Ashley Ave, Charleston, SC 29425, United States

Abstract

Post-traumatic stress disorder (PTSD) is a disabling psychological disorder characterized by chronic symptoms of intrusiveness, avoidance, and hyperarousal after a traumatic event. Retrospective studies have indicated PTSD increases the risk for cardiovascular disease (CVD) including arrhythmia, hypertension, and myocardial infarction. The goal of this study was to: 1) use a murine model of cued fear conditioning (inescapable foot shock, IFS) to develop a scoring

[*]Corresponding author at: Department of Medicine, Medical University of South Carolina, 30 Courtenay Drive, Charleston, SC 29425, United States., deleonky@musc.edu (K.Y. DeLeon-Pennell).

CRediT authorship contribution statement

Alexa Corker: Writing – review & editing, Writing – original draft, Visualization, Methodology, Investigation, Funding acquisition, Formal analysis, Data curation, Conceptualization. **Miguel Troncoso:** Writing – review & editing, Methodology. **Maya Learmonth:** Writing – review & editing, Methodology. **Philip Broughton:** Writing – review & editing, Methodology. **Sara J. Sidles:** Writing – review & editing, Supervision, Resources, Methodology, Formal analysis. **Ryan Kelly:** Writing – review & editing, Methodology, Formal analysis. **Shaoni Dasgupta:** Writing – review & editing, Methodology. **Thomas Dempster:** Writing – review & editing, Visualization, Formal analysis. **Kim Vu:** Writing – review & editing, Methodology, Formal analysis. **Amber Hazzard:** Writing – review & editing, Methodology. **An Van Laer:** Writing – review & editing, Supervision, Methodology. **Rachel D. Penrod:** Writing – review & editing, Supervision, Methodology, Data curation. **Jeffery A. Jones:** Writing – review & editing, Methodology. **Amy D. Bradshaw:** Writing – review & editing, Methodology. **Michael R. Zile:** Writing – review & editing, Methodology, Data curation. **Amanda C. LaRue:** Writing – review & editing, Validation, Methodology, Data curation. **Kristine Y. DeLeon-Pennell:** Writing – review & editing, Writing – original draft, Visualization, Validation, Supervision, Resources, Project administration, Investigation, Funding acquisition, Data curation, Conceptualization.

method to distinguish a PTSD-like phenotype, and 2) use this model system to characterize the cardiac phenotype and function in mice with extreme PTSD-like behaviors. We compared 3 groups, controls, non-responders (NR), and PTSD-like mice at 2 time points [4-weeks and 8-weeks post-IFS] to compare left ventricular structure and function. Assessment of cardiac function showed both male and female PTSD-like mice had increased isovolumetric relaxation time at 8-weeks post-IFS, whereas only females demonstrated increases in E/e', left atrial diameter, and decreased ejection fraction compared to control mice. Female PTSD-like mice also demonstrated increased interstitial fibrosis through picrosirius red staining and increased expression of fibrotic genes including *Col3a1* and *Lox*. Overall, our data indicated that mice displaying behavioral characteristics associated with PTSD present with sex-dependent diastolic dysfunction likely due, at least in part, to an activation of cardiac fibrosis.

Keywords

Inflammation; Fibrosis; Cardiovascular disease; Fear-conditioning; Sex difference; Heart failure

1. Introduction

Post-traumatic stress disorder (PTSD) is a disabling psychological disorder characterized by chronic symptoms of intrusiveness, avoidance, and hyperarousal after a traumatic event. Patients diagnosed with PTSD have a two-times higher risk of experiencing an adverse cardiac event like myocardial infarction or stroke compared to patients without PTSD even after adjustment for confounding factors like diabetes, hypertension, and depression [1–5]. While the mechanism behind this risk is unknown, chronic and uncontrolled inflammation is often reported with mental disorders and pathologies likely contributing to cardiovascular disease (CVD) risk [6]. Clinical studies have demonstrated that PTSD etiology has downstream functional effects on the immune system, which may affect cardiovascular remodeling and function [7–12]. While there are multiple clinical studies addressing a correlation between PTSD and CVD outcomes, studies investigating the reason for the connection between PTSD and CVD are few.

Use of rodent models to simulate aspects of PTSD such as the social-defeat and predator scent stress models have demonstrated that long-term alterations in heart rate variability and myocyte function occur in PTSD animals [13,14]; however, there remains a significant need to examine chronic effects on cardiac structure and remodeling beyond basic cardiovascular parameters. The animal variability seen in PTSD murine studies represents the heterogeneous clinical presentation of PTSD. Despite this strength, variability within experimental groups has prevented a clear and translatable conclusion regarding the impact of PTSD on cardiovascular health. While most previously studied models reliably produce generalized anxiety- and/or depression-like behaviors, specific constructs like arousal were variable across parameters and were not consistent [15]. In addition, many previously studied models were optimized for male behavioral phenotypes and disregarded female behavior due to increased variability, limiting our understanding of female behaviors associated with fear-conditioning [15].

In the last decade, the animal behavior field has demonstrated the strength of using composite *Z*-scores for multidimensional behavioral testing to control for subject variability [16,17]. A single behavior test for animal models is not sufficient to assess the multiple aspects of trauma and is not consistent with the clinical concept of PTSD. Due to variability of behavioral tests (e.g., lower scores for some behavioral tests indicate better performance, and in others, higher scores are better), simple addition or averaging of the different tests does not accurately reflect mouse phenotype. Use of test batteries that cover multiple diagnostic criteria and time points may provide insight into the direct effects of stress over time while controlling for subject variability.

Accordingly, we hypothesized that use of a multiple diagnostic criteria to characterize mice as a PTSD-like phenotype will elucidate novel regulators of PTSD-associated adverse cardiac remodeling and cardiac dysfunction observed in the clinical population. By considering individual variability, we aimed to generate a reproducible model that will allow us to evaluate symptom severity and further dissect the cardiovascular phenotype present in a PTSD-like behavioral phenotype.

2. Methods

2.1. Animal assurance for prospective experiments

All animal procedures were approved by the Institutional Animal Care and Use Committee at Ralph H. Johnson VA Medical Center in accordance with the Guide for the Care and Use of Laboratory Animals and followed the ARRIVE guidelines [18]. Male and female mice (C57BL/6 J) were separated into 6 cohorts, each containing controls (4-weeks: males: 4.9 ± 0.3 months of age; females: 4.7 ± 0.1 months of age; 8-weeks: males: 6.0 ± 0.2 months of age; females: 6.1 ± 0.2 months of age) and mice that undergo the inescapable foot shock (IFS) model (4-weeks: males: 4.8 ± 0.1 months of age; females: 4.7 ± 0.1 months of age; 8-weeks: males: 6.0 ± 0.1 months of age; females: 6.3 ± 0.1 months of age). All mice were bred in house and kept in a light-controlled environment with a 12-h:12-h light/dark cycle and given free access to standard mouse chow and water. Mice were group housed throughout the experiments unless behavioral testing required single housing temporarily.

2.2. Cued Fear-Conditioning (Inescapable Foot Shock; IFS)

Mice were randomly selected and underwent a cued fear-conditioning protocol (inescapable foot shock; IFS) [19]. Mice were placed in a fear-conditioning chamber (Ugo Basile) for 6 min where they were exposed to 5 foot shocks (1.0 mA). Mice were exposed to a 19 s tone as the trauma association (9000 hz, 80 % intensity), before receiving a 1 s foot shock. Tone terminated prior to mice receiving foot shock. Aged-matched control mice underwent a 6-min trial period where a 19 s tone (9000 hz, 80 % intensity) was played but foot shock was not received. Video data was collected by an overhead high-speed camera (25 frames per second) and reviewed using EthoVision XT (Noldus). Cued fear-conditioning was initiated between 9 and 10 am.

2.3. Behavioral tests for PTSD-like mice

To characterize behavioral phenotypes, we developed a composite *Z*-score that incorporates multiple behavioral tests (Table 1, Supplementary Figs. 1–5). Each assessment was uniquely chosen to match specific PTSD criteria as detailed in the DSM–5 (Diagnostic and Statistical Manual of Mental Disorders). To adjust for potential effects of the repetitive tests at different time points, we calculated behavioral parameters values from each test as a fold change of the parameter measured at baseline before IFS (week 0; pre-IFS, $n = 20$ parameters) versus terminal collection (week 4- or 8-post-IFS). All tests for baseline and terminal time points were performed in a temperature-controlled room at the same time of day to remove any influence of circadian rhythm. Mice were also habituated for a minimum of 20 min in testing rooms prior to the start of the tests. Based on outputs from behavioral testing, IFS mice were classified as either non-responders (NR), mice that are resilient to IFS, (NR; 4-weeks: males = 8; females = 9; 8-weeks: males = 8; females = 4) or PTSD-like, mice that are susceptible to IFS (4-weeks: males = 9; females = 12; 8-weeks: males = 4; females = 5).

2.4. Composite Z-score

To interpret behavioral results, we incorporated cut-off behavioral criteria and clustering methods similar to what is used in the clinic for the classification of susceptible and resilient trauma-exposed individuals [20]. From the 6 behavioral tests performed, 20 parameters (Table 1) were selected due to minimal variation and consistency over time within the control group. Description of all behavioral methods used to generate composite scores are detailed in the Supplemental Methods. We calculated a composite Z score for each behavioral parameter, as follows: $Z = (x - u)/\sigma$ (x= fold change, u = control average, σ = control standard deviation) [21]. Fold change of each behavioral parameter was calculated by dividing terminal time point values by baseline values for each individual mouse. Each cohort included control mice (no IFS) that underwent the same behavioral tests as the IFS mice to set the limits for scoring. Scores were calculated using the control mice within the same cohort. The absolute value of the *Z*-score for each behavioral parameter within individual symptom clusters were averaged and the overall composite Z-score was then calculated by averaging the scores for each symptom cluster, so that individual cluster(s) or parameter(s) are weighted equally. Cutoff values were determined as follows: *average* + (2 × *Standard Deviation*). To be classified as PTSD-like, mice must demonstrate at minimum a composite Z-score greater than the cut-off value for the overall score in addition to 3 of the 4 symptom clusters (intrusiveness, social avoidance, negative mood/cognition, hyperarousal; Supplementary Fig. 1). Based on the composite score, IFS mice that did not meet all the criteria to be considered PTSD-like were classified as NR.

2.5. Echocardiography

Serial echocardiography and doppler imaging were collected at weeks 0-, 2-, 4-, and 8-weeks post-IFS (Vevo 3100, VisualSonics; Toronto, CA) following recommendations published in the “Guidelines For Measuring Cardiac Physiology in Mice” [22,23]. During the echocardiography procedure, mice were anesthetized with 1.0–1.5 % isoflurane in oxygen mix. Electrocardiogram, heart rate, and body temperature were monitored during the imaging procedure. All images were acquired at heart rates >400 beats/min for

physiologically relevant measurements. Measurements were taken from the left ventricle (LV) parasternal long-axis and pulse wave flow and tissue velocity doppler of the pulmonary and mitral valve using integrated VevoLAB software. For all echocardiographic variables, 3 images from consecutive cardiac cycles were measured and averaged for final reporting. For doppler outputs, 5 consecutive cardiac cycles were measured and averaged.

2.6. Tissue collection

For euthanasia, mice were anesthetized with 1.5–2.0 % isoflurane in an oxygen mix. During tissue collection, heparin (1000 USP/mL) was injected intraperitoneally, and blood was collected from the carotid artery. The blood was centrifuged for 5 min to separate out plasma, and 1× proteinase inhibitor (Roche, 1169749800) was added before snap freezing in liquid nitrogen. Hearts were excised and flushed with cardioplegic solution (69 mM NaCl; 12 mM NaHCO3; 11 mM glucose; 30 mM 2,3-butanedione monoxime; 10 mM EGTA; 0.001 mM Nifedipine; 50 mM KCl; and 100 U Heparin in 0.9 % saline, pH 7.4) to arrest the heart in diastole. The LV was separated from the right ventricle and individually weighed. The LV was cut into three equal sections: base, mid-papillary, and apex. The base and apex were individually snap frozen in liquid nitrogen and stored in −80 °C for later use. The mid-papillary section was fixed in zinc formalin fixative (Sigma Aldrich, Z2902) and embedded in paraffin for histological staining.

2.7. Histology

For histological analysis, tissue samples underwent deparaffinization and rehydration before heat-mediated antigen retrieval (Target Retrieval Solution, Dako S1699) was performed to expose target antigens. No antigen retrieval was performed for wheat germ agglutin (WGA) staining. Blocking serum was then applied (Mac3-Rabbit Serum; Vector Laboratories, S-5000; WGA-Goat Serum, Vector Laboratories, S-1000) and slides were left to incubate for 1 h at room temperature. After blocking, either Mac-3 primary antibody (Cedarlane CL8943AP; 1:100) or WGA-AlexaFluor488 conjugate (Invitrogen, W11261, 1:200) was added. For Mac-3 staining, tissue was incubated in primary antibody overnight at 4 °C followed by rabbit anti-rat IgG secondary antibody (Rabbit anti-rat IgG, Vector Laboratories, PK-6104) for 1 h at room temperature. HistoMark Black (SeraCare, 5510-0034) was used to visualize positive Mac-3 staining, with eosin as a counterstain. Negative controls with no Mac-3 antibody were used. Slides with WGA stain were incubated for 2 h at room temperature. TrueBlack (Biotium, 23007) was added for 1 min to limit tissue auto fluorescence. DAPI Mounting Media (Vectashield, H-1200) was then added to visualize nuclei. To visualize collagen, slides were incubated in 0.2 % phosphomolybdic acid (Electron Microscopy Sciences, RT 26357-01) for 3 min followed by 0.1 % Sirius Red in saturated picric acid (Electron Microscopy Sciences, RT 26357-02) for 90 min. Immediately after, slides were placed into acidified water for 2 min. For all staining protocols, 10–20 images were captured on Echo Revolve Microscope or Olympus Model BX43 Trinocular Research Microscope at 40× magnification for each LV section. Scans of the LV were taken to record both perivascular and interstitial fibrosis. Images were collected so that at minimum 10 contained staining of large intramyocardial vessels to represent perivascular fibrosis and 10 images without visible vessels to represent interstitial fibrosis.

The percentage of positive staining per field of view and cardiomyocyte area was calculated using Image-Pro version 10.0.11 (Media Cybernetics).

2.8. Protein isolation

The LV of control, NR, and PTSD-like mice were fractionated into soluble and insoluble fractions. Protein was extracted from LV tissue by homogenizing the samples sequentially in phosphate buffered saline (PBS) with 1× protease inhibitor cocktail (16 μL per mg tissue, soluble protein fraction), followed by protein extraction reagent type 4 (Sigma; 7 M urea, 2 M thiourea, 40 mM Trizma® base and the detergent 1 % C7BzO, 16 μL per mg tissue) with 1× protease inhibitor cocktail (insoluble protein fraction). Protein concentrations were determined by the Quick Start™ Bradford Protein Assay (Bio-Rad).

2.9. Proteomics

Assays for MMP-9 activity (Enzo, BML-AK410, 1:5 dilution of plasma, no dilution of insoluble protein fraction of the LV), circulating CCL2 levels (R&D Systems, MJE00B, 1:10 dilution), and circulating cardiac troponin I (Novus Biologicals, NBP3-00456, 1:2 dilution) were performed according to manufacturer instructions. Snap frozen plasma and insoluble protein fraction of the LV were thawed on ice and all samples were read in duplicate. Absorbance was read at wavelength specified by the manufacturer using the SpectraMax 190 microplate spectrophotometer microplate reader.

2.10. Gene expression

RNA was isolated from the LV of mice following RNeasy Mini Kit instructions (Qiagen, 74104). RNA levels were quantified using the NanoDrop ND-1000 Spectrophotometer (Thermo Scientific). Reverse transcription of equal RNA content (1 μg) was performed using the QuantiTect Reverse Transcription Kit (Qiagen, 205313). QuantiNova LNA Probe PCR focus panels on murine fibrotic markers (Qiagen, 249955) were used to quantify mRNA levels in LV tissue. QuantiNova Probe PCR kit was used to make the master mix for the focus panels (Qiagen, 208256). Thresholds were set based on the internal plate control (PPC) to remove plate to plate variability according to manufacturer's instructions. Ct values were normalized to the *B2m* housekeeping gene. Calculations for the ΔCt values was done using the Qiagen GeneGlobe Analysis software and manual calculations were performed by normalizing values to control (non IFS) values to determine $2^{-\Delta\Delta Ct}$. Differentially expressed genes identified underwent autoscaling by dividing the mean center by the standard deviation of each variable for bioinformatic and pathway analysis.

2.11. Cardiac macrophage phenotyping

RNAscope Multiplex Fluorescent kit was performed following v2 User Manual (ACDbio, 323280). Tissue samples were cut in an RNAse free environment 1–2 days prior to running RNAscope. Manual target retrieval was performed based on the manufacturer's instructions (Appendix B. in v2 User Manual) for 15 min followed by protease plus treatment for 15 min at room temperature. TSA Vivid Fluorophore 520 (Tocris Bioscience, 323271), TSA Vivid Fluorophore 570 (Tocris Bioscience, 323272), and TSA Vivid Fluorophore 650 (Tocris Bioscience, 323273) were used to visualize mRNA probes *CD86* (ACDbio,

403441-C3), *Ccr2* (ACDbio, 501681), and *CD206* (ACDbio, 437511-C2) respectively. TSA Vivid Fluorophores were diluted 1:750 in TSA buffer. Positive and negative control sections were performed for every sample assayed to determine mRNA presence/quality in tissue and probe specificity. Samples were excluded if positive control had limited mRNA staining. Sections were imaged at 20× within a week of assay on the A1Rsi Laser Scanning Nikon Confocal. Percent overlap was performed on a minimum of 5 images per sample using Image-Pro version 10.0.11 (Media Cybernetics). All representative images are shown at 20× with inserts by 2× digital zoom of the acquired images.

2.12. Bioinformatics and pathway analysis

Bioinformatic and pathway enrichment analysis was performed using tools available on the Metaboanalyst 6.0 package (www.metaboanalyst.ca/) [24]. Gene data was uploaded to Metaboanalyst as $2^{-\Delta\Delta Ct}$ and a one-way ANOVA with Tukey's post hoc test was performed separately for each sex to determine differentially expressed genes (defined as false discovery rate (FDR) adjusted $p < 0.05$). Partial least squares discriminant analysis (PLS-DA) was used for assessment of distribution and generating the Variable Importance in Projection or VIP score. The VIP score is a weighted sum of squares of the PLS weight, which indicates the importance of the genetic variable to the whole model. For generation of volcano plots, a fold change threshold of ±2.0 compared to sex-matched controls and a *p*-value of <0.05 based on FDR was used to compare gene expression between controls and post-IFS groups (NR and PTSD-like). Pathway impact score is based on the combination of the centrality and pathway enrichment results and was calculated by adding up the importance measures of each of the matched genes and then dividing by the sum of the importance measures of all genes within each pathway. Fisher's exact test was used for pathway enrichment with degree centrality being used for topology measurement.

2.13. Statistics

All statistical analyses were performed by investigators blinded to groups. Data are presented as means ± SEM. Multiple group comparisons were analyzed using two-way ANOVA, followed by the Bonferroni post-hoc test when the Bartlett's variation test passed, or the nonparametric Friedman test, followed by Dunn post hoc test when the Bartlett's variation test did not pass. A Pearson correlation coefficient was calculated to assess the linear relationship between interstitial fibrosis and behavioral parameters. All data has been separated by sex. Statistical significance was set at $p < 0.05$.

3. Results

3.1. Female, but not male, PTSD-like mice present with decreased cardiac function 8-weeks post-IFS

Serial echocardiography and doppler measurements show male PTSD-like mice and NR mice of both sexes had a significant increase only in isovolumetric relaxation time (IVRT) compared to controls while female PTSD-like mice had a significant increase in IVRT, E/e', and left atrial diameter (LAD) and experienced a decrease in ejection fraction (EF) at 8-weeks (Fig. 1; Table 2). To determine if there was any effect on right ventricular function, we measured pulmonary artery acceleration time to ejection time (PATET) ratio

which showed no significant differences between phenotypes or sex ($p = 0.6552$) at 8-weeks post-IFS. Results indicate male PTSD-like mice and all NR mice display slight alterations in filling pressure that is not yet pathological while female PTSD-like mice display diastolic dysfunction at 8-weeks.

3.2. PTSD-like phenotype exacerbates cardiac remodeling in female PTSD-like mice

To determine molecular changes potentially responsible for driving the cardiac dysfunction observed in female PTSD-like mice at 8-weeks, we assessed for markers of myocyte injury at 4-weeks. Circulating cardiac troponin showed no differences between groups (Fig. 2A). Along with this, no differences were observed in cardiomyocyte size at 4-weeks as seen in WGA-stained images (Fig. 2B). Plasma levels of MMP-9 activity, a known marker of cardiac remodeling associated with PTSD [25,26] was not significant across groups (Fig. 2C), although an increased trend was seen in male PTSD-like mice ($p = 0.1511$). Similar to what was observed in circulation, MMP-9 activity in the left ventricle was not significant across groups but had an increased trend in male PTSD-like mice ($p = 0.1240$) compared to NR of the same sex and a decreased trend compared to female PTSD-like mice ($p = 0.1237$; Fig. 2D). Picrosirius red staining demonstrated an increase in male vascular collagen levels when compared to mice across all groups and sexes (Fig. 2E), which has been previously reported in aged mouse models [27]. In contrast, female PTSD-like mice had increased interstitial collagen compared to NR and controls (Fig. 2E). We conclude that increased interstitial fibrosis observed at 4-weeks likely contributes to diastolic dysfunction found in female PTSD-like mice at 8-weeks post-IFS. To determine if the degree of behavioral consequences after IFS set the heart on a path toward pathology and dysfunction, we performed correlations between specific behavioral parameters and interstitial fibrosis values measured at 4-weeks in the post-IFS groups (Table 3). Interstitial fibrosis was significantly correlated with session extinction coefficient scores in female PTSD-like mice ($r = 0.8989$; $p = 0.0380$) whereas duration spent in the middle zone during open field was correlated with interstitial fibrosis in male PTSD-like mice ($r = 0.8853$; $p = 0.0190$). In female NR mice, duration of the enrichment runway test was negatively correlated with interstitial fibrosis ($r = -0.7577$; $p = 0.0485$). While many of the other behavioral tests demonstrated trends, none were considered significant.

3.3. Male and female mice display differing left ventricular gene expression

To determine potential drivers in our PTSD-like mice at 4-weeks, we assessed for gene markers of fibrosis in LV tissue. PLSDA analysis of the gene array panels illustrated little overlap between groups indicating distinct clustering of the genetic data between the control, NR, and PTSD-like mice (Fig. 3A–B). As shown in the volcano plot, male NRs at 4-weeks post-IFS had increased expression of tissue growth factor-β1 (*Tgfb1*), endoglin (*Eng*), platelet derived growth factor-β (*Pdgfb*), bone-morphogenic protein-7 (*Bmp7*), glucuronidase-β (*Gusb*), plasminogen activator (*Plat*), and signal transducer and activator of transcription-6 (*Stat6*) when compared to male controls (Fig. 3C, Table 4). In contrast, male PTSD-like mice had decreased integrin alpha 3 (*Itga3*) and integrin alpha v (*Itgav*) expression compared to controls (Fig. 3D, Table 4). Compared to female controls, lysyl oxidase (*Lox*) was the only significantly upregulated gene in female NR mice (Fig. 3E, Table 4), whereas female PTSD-like mice expressed elevated levels of integrin beta 8

(*Itgb8*), collagen type 3 alpha 1 (*Col3a1*), and *Lox* at 4-weeks, reflective of the increased fibrotic deposition observed by PSR staining (Fig. 3F, Table 4). Variable importance in projection (VIP) analysis was used to weigh the significance of each variable to the whole model (Fig. 3G–H). Genetic variables with a VIP score > 2.0 were considered as potential drivers of the observed cardiac pathology (*labeled by stars*). In males, *Itga3* was identified as having the highest VIP score but with decreased genetic expression being observed in male PTSD-like mice compared to controls and NRs (Fig. 3G). In females, *Lox* was shown to have the highest VIP score with the highest expression levels observed in PTSD-like female mice (Fig. 3H).

To determine if these genetic changes were linked to functional or pathway enrichment, pathway analysis was performed. Male NR mice demonstrated an upregulation in genes associated with the AGE-RAGE, TGF-β, and proteoglycan signaling pathways (Fig. 4A). In contrast, male PTSD-like mice showed a downregulation of AGE-RAGE, TGF-β, and fluid sheer stress signaling (Fig. 4B). Female NR mice also demonstrated an elevation in genes associated with the TGF-β pathway along with an increase in complement and coagulation cascade and a downregulation in genes related to cytosolic/DNA sensing pathway (Fig. 4C). In contrast to males, female PTSD-like mice had a slight increase in AGE-RAGE and TGF-β signaling along with a similar decrease seen in male PTSD-like mice in genes associated with fluid sheer stress (Fig. 4D). Overall, our genetic assessment further stratified behavioral phenotypes seen in our composite score with a profibrotic signature observed in female PTSD-like mice. These clear-cut differences in genetic expression between sexes and groups may be leading to impairments in cardiac function in females.

3.4. Resident macrophages may be playing a role in PTSD induced cardiac dysfunction

Due to genetic data indicating the potential for modulations in the inflammatory response, we tested macrophage numbers between groups. Histological staining of the LV showed an increased trend ($p = 0.0542$) but no significant differences in macrophages within the LV of male PTSD-like mice compared to respective controls 4-weeks after IFS (Fig. 5A). No differences were observed in female mice between groups. Despite there being no difference in total macrophage numbers, an assessment of potential impact of recruited monocyte-derived macrophages at 4-weeks post-IFS was performed. We first assessed for a known monocyte chemotactic protein, CCL2, and found no difference in circulating CCL2 between the groups at 4-weeks post-IFS (Fig. 5B). We then measured markers of monocytes and macrophage phenotypes via in situ hybridization. Interestingly, *Ccr2* mRNA expression decreased in male and female NR and PTSD-like mice when compared to controls (Fig. 5C). No differences were reported with colocalization of *Ccr2* + *CD86*+ and *Ccr2* + *CD206*+ mRNA positive macrophages in the PTSD-like group of either sex (Fig. 5C). Female NR had an increase in *Ccr2* + *CD86* colocalization compared to female controls indicating inflammation likely has a minor role in diastolic impairment observed in female PTSD-like mice.

4. Discussion

The goals of this study were twofold: 1) use a murine model of cued fear conditioning (inescapable foot shock, IFS) to develop a scoring method to distinguish a PTSD-like phenotype, and 2) use this model system to characterize cardiac phenotype and function in mice with PTSD-like symptoms. Using our behavioral scoring method, we were able to separate out a group of mice that demonstrated an exaggerated behavioral phenotype 4- and 8-weeks after IFS that we labeled as PTSD-like. With our refined method of PTSD-like behavior evaluation, we found sex dependent differences in behavioral output and cardiovascular function in mice after cue-associated fear conditioning. To our knowledge, our study is one of the first to demonstrate an adverse cardiac phenotype in a subset of female mice displaying a PTSD-like behaviors, which is most likely due to increased fibrotic deposition.

Clinical studies have shown innate sex differences reported in PTSD diagnosis rates, symptom severity and duration of symptoms [28,29]. Women are typically protected from cardiac events until menopause, while men have a higher risk of experiencing a cardiac event when compared to aged-matched women [30,31]. The mice in our study are considered middle aged and so we originally hypothesized that female mice would be protected due to the beneficial cardiovascular effects of female hormones. At first, we were surprised our female PTSD-like mice had clearer signs of cardiac dysfunction at the time points examined than the male PTSD-like mice however, when assessing clinical literature we found that in the absence of hypertension, women with PTSD had diastolic dysfunction compared to healthy aged matched women as indicated by increased E/e’ ratio similar to what we observe in our female PTSD-like mice [32]. Female NR and male PTSD-like mice did not show signs of significant cardiac dysfunction; however, both groups had an increase in IVRT suggesting impaired LV filling. There is limited literature investigating how PTSD-like symptomology in mice can influence the cardiac environment and the possible mechanisms behind it. These results, to our knowledge, are the first to demonstrate a female dominant cardiac phenotype in a murine model of PTSD.

Our behavioral tests demonstrated different behavioral outputs between male and female mice after cue-associated fear conditioning at 4- and 8-weeks. The strength of the IFS model is the heterogeneity in the behavioral responses mimicking the clinical population however, due to the variability in the animals response, some studies have been inconclusive in regard to the cardiac phenotype [33–35]. By integrating a scoring method, we aimed to pull out the more extreme behavioral phenotypes to identify key signatures that may be driving the cardiovascular pathology associated with PTSD. Male PTSD-like mice behaviors appeared to persist over longer periods, although were highly variable, with some animals showing signs of hyperarousal while others demonstrated the opposite. Female PTSD-like mice appeared to have less variability in their behavioral data and were characterized by a continued anxiety-like phenotype. Changes in behavior in chronic stress models have been reported in male mice previously by other groups, but female behavioral data is understudied [36]. It is possible that due to the limited data in females, the cardiac phenotype may have been overlooked. More recent clinical studies have demonstrated premenopausal women with a PTSD diagnosis exhibited an exaggerated increase in blood pressure and heart rate

during a cold-pressor test suggesting an overactive sympathetic and hemodynamic response [37]. These clinical findings are in line with our study and provide a potential explanation for the propensity toward developing cardiovascular disease later in life in young women, who are typically thought to be protected from CVD.

No changes in circulating cardiac troponin, LV weight, and myocyte size were observed in either sex at 4-weeks post-IFS, suggesting cardiomyocytes alone may not be the early driver of cardiac dysfunction observed in our model. With diastolic impairment, there typically is an associated interstitial fibrotic collagen deposition and extracellular matrix remodeling [38,39]. Increased interstitial fibrosis in the LV can lead to stiffening of the ventricle and decreased cardiac function. Female PTSD-like mice reflected this molecular pathology and had increased interstitial fibrosis while male PTSD-like mice did not. Similarly, female PTSD-like mice also had increased *Col3a1* and *Lox* gene expression in the LV. Lox is an enzyme that facilitates in collagen cross-linking and tissue stiffening [40–43]. Future studies evaluating matrix organization and cardiac stiffness in our model will reveal if these genetic changes were key in the pathology observed in our female PTSD-like mice.

While we were able to identify molecular differences between PTSD-like and NR groups, it is unclear what exactly is protecting the NR group from having an exaggerated behavioral and cardiac phenotype. Of interest, male NRs had an increase in genes within the Tgfβ superfamily including *Tgfb1*, *Eng*, and *Bmp7*. The Tgfβ superfamily regulates cell survival, differentiation, and proliferation and different aspects of the reparative response including angiogenesis and fibrosis, implicating this increase as a potential protective mechanism [44,45]. In female NR mice, only *Lox* gene expression was identified to be significantly different than controls. As discussed above, *Lox* expression was also elevated in PTSD-like mice but to a greater extent than what was observed in NR mice. Future studies investigating potential stress hormones and neurological mechanisms that may be stimulating these molecular differences between the NR and PTSD-like groups is needed to identify potential protective mechanisms that could be exploited as a therapy.

Due to the nature of clinical diagnosis, patients are not considered to have PTSD until the patient has experienced a minimum of 1 month of symptoms. The same metric is used in the model summarized here. Because of this, we did not investigate the acute molecular changes before the 1-month time point which limited our understanding of what basic mechanisms could be reflective immediately after trauma in this study. For future studies, we plan to include earlier blood draws to track changes in inflammation and immune cell populations prior to the termination of the study.

For this study, we also focused solely on the left ventricle as our pulmonary doppler measurements did not indicate right ventricular dysfunction. Our study also performed minimal investigation into the vasculature and possible hypertension in our PTSD-like mice. We expect that PTSD-like mice will have increased blood pressure compared to control mice, likely contributing to the impairment in cardiac function. Previous studies using a similar fear-conditioning model showed stress-dependent increases in blood pressure that were blunted after AT1R inhibition with losartan [46]. Interestingly, sequencing of the basolateral amygdala showed a downregulation of differentially expressed genes in

the losartan group that were primarily linked to metabolic processes and inflammation. Further investigation is needed into autonomic nervous system outputs like blood pressure, resting heart rate, and heart rate variability in PTSD murine models. Future experiments investigating the effects of vagal nerve stimulation on cardiac function and possible effects on fibrosis and fibroblast activation would support the association of autonomic dysfunction in PTSD and cardiovascular outcomes. Studies using the repeated social defeat stress model have been shown to alter the systemic immune profile likely contributing to adverse outcomes in both behavior and cardiac function [47,48]. Our study also pointed to a potential inflammatory mediated mechanism specifically in males. While not observed in female PTSD-like mice, male PTSD-like mice had an increased trend in macrophage numbers in the LV. Surprisingly, *Ccr2* expression was decreased and no significant changes were seen with circulating CCL2 levels in any of the groups, leading us to believe that resident macrophages, not monocyte derived macrophages, are likely contributing to the early signs of LV dysfunction seen in male PTSD-like mice. Male PTSD-like mice also had a decrease in *Itga3* and *Itgav* gene expression, contributing to the idea that immune cell recruitment is downregulated in male PTSD-like mice [49,50]. Intriguingly, female NR mice had an increase in the number of *Ccr2* + *CD86*+ *cells*, representative of an increase in pro-inflammatory monocytes. This may add to previous studies showing how chronic stress primes monocytes, leading to higher risk of adverse outcomes following a second event like infection or myocardial infarction [51]. Further investigation is needed into how transcriptional programming of monocytes/macrophages from PTSD-like and NR mice are contributing to PTSD-phenotypic severity and cardiac dysfunction. Additional studies evaluating the immune profile in our model and how these cells may be contributing to disease would increase our understanding of PTSD-associated CVD outcomes.

In conclusion, using the scoring method to cluster based on PTSD-like phenotypic severity, we were able to identify potential mechanisms responsible for diastolic dysfunction in female PTSD-like mice. Interestingly, male and female mice exhibited differing behavioral and molecular patterns post-IFS implicating divergent processes activated in response to trauma. Our research establishes a cardiac phenotype present in a cued fear conditioning IFS model and provides a platform to discover possible pathological contributions to clinical associations between PTSD and CVD in women.

Supplementary Material

Refer to Web version on PubMed Central for supplementary material.

Acknowledgements

K.Y.D.-P. and A.C. conceived and designed research; A.C., M.T., M.L., P.B., S.D., T.D., K.V., A.H., T.D. performed experiments; A.C., S.S., R.K., J.J., A.L., K.Y.D.-P. designed the modified foot shock protocol, A.C., S.S., R.K., R.P., A.L., K.Y.D.-P analyzed and interpreted behavioral data; A.C., A.VL., M.Z., K.Y.D.-P collected and analyze echocardiography data; A.C. and K.Y.D.-P. analyzed data and interpreted results of all experiments; A.C. and K.Y.D.-P. prepared figures and drafted manuscript; A.C., M.T., M.L., P.B., S.S., R.K., S.D., T.D., K.V., A.H., A.VL., R.P., J.J., A.B., M.Z., A. L., K.Y.D.-P. edited and approved of manuscript.

This research was supported in part by the VA Shared Resource Program (Small Animal Behavioral & Physiological Assessment Core, Small Animal Imaging Core, and Cellular & Molecular Evaluation Core) at the Ralph H. Johnson VA Health Care System.

The authors did not use generative AI or AI-assisted technologies in the development of this manuscript.

Funding

This work was supported by the American Heart Association 24PRE1188095; National Institutes of Health, F31HL170740, GM113278, T32GM123055, T32GM152386, P20GM148302 and HL173273; the Biomedical Laboratory Research and Development Service of the Veterans Affairs Office of Research and Development Award I01BX00584; and by the National Center for Advancing Translational Sciences TL1TR001451 & UL1TR001450. The content is solely the responsibility of the authors and does not necessarily represent the official views of the National Institutes of Health, American Heart Association, or Veteran Affairs.

References

[1]. Remch M, Laskaris Z, Flory J, Mora-McLaughlin C, Morabia A, Post-traumatic stress disorder and cardiovascular diseases: a cohort study of men and women involved in cleaning the debris of the world trade center complex, Circ. Cardiovasc. Qual. Outcomes 11 (7) (2018) e004572. [PubMed: 29991645]

[2]. Turner JH, Neylan TC, Schiller NB, Li Y, Cohen BE, Objective evidence of myocardial ischemia in patients with posttraumatic stress disorder, Biol. Psychiatry 74 (11) (2013) 861–866. [PubMed: 23978403]

[3]. Roy SS, Foraker RE, Girton RA, Mansfield AJ, Posttraumatic stress disorder and incident heart failure among a community-based sample of US veterans, Am. J. Public Health 105 (4) (2015) 757–763. [PubMed: 25713943]

[4]. Kubzansky LD, Koenen KC, Jones C, Eaton WW, A prospective study of posttraumatic stress disorder symptoms and coronary heart disease in women, Health Psychol. 28 (1) (2009) 125–130. [PubMed: 19210026]

[5]. Sumner JA, Kubzansky LD, Elkind MS, Roberts AL, Agnew-Blais J, Chen QM, et al. , Trauma exposure and posttraumatic stress disorder symptoms predict onset of cardiovascular events in women, Circulation 132 (4) (2015) 251–259. [PubMed: 26124186]

[6]. Lauten TH, Natour T, Case AJ, Innate and adaptive immune system consequences of post-traumatic stress disorder, Auton. Neurosci. 252 (2024) 103159. [PubMed: 38428324]

[7]. Katrinli S, Oliveira NCS, Felger JC, Michopoulos V, Smith AK, The role of the immune system in posttraumatic stress disorder, Transl. Psychiatry 12 (1) (2022) 313. [PubMed: 35927237]

[8]. Sun Y, Qu Y, Zhu J, The relationship between inflammation and post-traumatic stress disorder, Front. Psychol. 12 (2021) 707543.

[9]. Altemus M, Cloitre M, Dhabhar FS, Enhanced cellular immune response in women with PTSD related to childhood abuse, Am. J. Psychiatry 160 (9) (2003) 1705–1707. [PubMed: 12944352]

[10]. O'Donovan A, Cohen BE, Seal KH, Bertenthal D, Margaretten M, Nishimi K, et al. , Elevated risk for autoimmune disorders in Iraq and Afghanistan veterans with posttraumatic stress disorder, Biol. Psychiatry 77 (4) (2015) 365–374. [PubMed: 25104173]

[11]. Cohen M, Meir T, Klein E, Volpin G, Assaf M, Pollack S, Cytokine levels as potential biomarkers for predicting the development of posttraumatic stress symptoms in casualties of accidents, Int. J. Psychiatry Med. 42 (2) (2011) 117–131. [PubMed: 22409092]

[12]. Toft H, Bramness JG, Lien L, Abebe DS, Wampold BE, Tilden T, et al. , PTSD patients show increasing cytokine levels during treatment despite reduced psychological distress, Neuropsychiatr. Dis. Treat. 14 (2018) 2367–2378. [PubMed: 30271153]

[13]. Koresh O, Kaplan Z, Zohar J, Matar MA, Geva AB, Cohen H, Distinctive cardiac autonomic dysfunction following stress exposure in both sexes in an animal model of PTSD, Behav. Brain Res. 308 (2016) 128–142. [PubMed: 27105958]

[14]. Finnell JE, Muniz BL, Padi AR, Lombard CM, Moffitt CM, Wood CS, et al. , Essential role of ovarian hormones in susceptibility to the consequences of witnessing social defeat in female rats, Biol. Psychiatry 84 (5) (2018) 372–382. [PubMed: 29544773]

[15]. Deslauriers J, Toth M, Der-Avakian A, Risbrough VB, Current status of animal models of posttraumatic stress disorder: behavioral and biological phenotypes, and future challenges in improving translation, Biol. Psychiatry 83 (10) (2018) 895–907. [PubMed: 29338843]

[16]. Matsumura K, Kumar TP, Guddanti T, Yan Y, Blackburn SL, McBride DW, Neurobehavioral deficits after subarachnoid hemorrhage in mice: sensitivity analysis and development of a new composite score, J. Am. Heart Assoc. 8 (8) (2019) e011699. [PubMed: 30971151]

[17]. Peng M, Zhang C, Dong Y, Zhang Y, Nakazawa H, Kaneki M, et al. , Battery of behavioral tests in mice to study postoperative delirium, Sci. Rep. 6 (2016) 29874. [PubMed: 27435513]

[18]. Kilkenny C, Browne WJ, Cuthill IC, Emerson M, Altman DG, Improving bioscience research reporting: the ARRIVE guidelines for reporting animal research, PLoS Biol. 8 (6) (2010) e1000412. [PubMed: 20613859]

[19]. Sidles SJ, Kelly RR, Kelly KD, Hathaway-Schrader JD, Khoo SK, Jones JA, et al. , Inescapable foot shock induces a PTSD-like phenotype and negatively impacts adult murine bone, Dis. Model. Mech. 17 (1) (2024).

[20]. Verbitsky A, Dopfel D, Zhang N, Rodent models of post-traumatic stress disorder: behavioral assessment, Transl. Psychiatry 10 (1) (2020) 132. [PubMed: 32376819]

[21]. Andrade C, Scores Z, Standard Scores, and composite test Scores explained, Indian J. Psychol. Med. 43 (6) (2021) 555–557. [PubMed: 35210687]

[22]. Lindsey ML, Kassiri Z, Virag JAI, de Castro Bras LE, Scherrer-Crosbie M, Guidelines for measuring cardiac physiology in mice, Am. J. Physiol. Heart Circ. Physiol. 314 (4) (2018) H733–H752. [PubMed: 29351456]

[23]. Thibault HB, Kurtz B, Raher MJ, Shaik RS, Waxman A, Derumeaux G, et al. , Noninvasive assessment of murine pulmonary arterial pressure: validation and application to models of pulmonary hypertension, Circ. Cardiovasc. Imaging 3 (2) (2010) 157–163. [PubMed: 20044514]

[24]. Xia J, Sinelnikov IV, Han B, Wishart DS, MetaboAnalyst 3.0–making metabolomics more meaningful, Nucleic Acids Res. 43 (W1) (2015) W251–W257. [PubMed: 25897128]

[25]. Chevalier CM, Krampert L, Schreckenbach M, Schubert CF, Reich J, Novak B, et al. , MMP9 mRNA is a potential diagnostic and treatment monitoring marker for PTSD: evidence from mice and humans, Eur. Neuropsychopharmacol. 51 (2021) 20–32. [PubMed: 34022747]

[26]. Xia Y, Wehrli J, Abivardi A, Hostiuc M, Kleim B, Bach DR, Attenuating human fear memory retention with minocycline: a randomized placebo-controlled trial, Transl. Psychiatry 14 (1) (2024) 28. [PubMed: 38233395]

[27]. DuPont JJ, Kim SK, Kenney RM, Jaffe IZ, Sex differences in the time course and mechanisms of vascular and cardiac aging in mice: role of the smooth muscle cell mineralocorticoid receptor, Am. J. Physiol. Heart Circ. Physiol. 320 (1) (2021) H169–H180. [PubMed: 33095647]

[28]. Fonkoue IT, Michopoulos V, Park J, Sex differences in post-traumatic stress disorder risk: autonomic control and inflammation, Clin. Auton. Res. 30 (5) (2020) 409–421. [PubMed: 33021709]

[29]. Soegaard EGI, Kan Z, Koirala R, Hauff E, Thapa SB, Gender differences in a wide range of trauma symptoms after victimization and accidental traumas: a cross-sectional study in a clinical setting, Eur. J. Psychotraumatol. 12 (1) (2021) 1975952. [PubMed: 34603637]

[30]. Rodgers JL, Jones J, Bolleddu SI, Vanthenapalli S, Rodgers LE, Shah K, et al. , Cardiovascular risks associated with gender and aging, J. Cardiovasc. Dev. Dis. 6 (2) (2019).

[31]. Pullen AB, Kain V, Serhan CN, Halade GV, Molecular and cellular differences in cardiac repair of male and female mice, J. Am. Heart Assoc. 9 (8) (2020) e015672. [PubMed: 32295449]

[32]. Hieda M, Yoo JK, Badrov MB, Parker RS, Anderson EH, Wiblin JL, et al. , Reduced left ventricular diastolic function in women with posttraumatic stress disorder, Am. J. Phys. Regul. Integr. Comp. Phys. 317 (1) (2019) R108–R112.

[33]. McCarty R, Cardiovascular responses to acute footshock stress in adult and aged Fischer 344 male rats, Neurobiol. Aging 6 (1) (1985) 47–50. [PubMed: 4000385]

[34]. McCarty R, Baucom K, Physiological responses of rats to footshock stress: effects of social environment, Behav. Neural Biol. 34 (4) (1982) 394–403. [PubMed: 7126089]

[35]. Nyakas C, Balkan B, Steffens AB, Bohus B, Cardiac and behavioral responses of long-term obese and lean Zucker rats to emotional stress, Physiol. Behav. 58 (6) (1995) 1079–1084. [PubMed: 8623005]

[36]. Tran I, Gellner AK, Long-term effects of chronic stress models in adult mice, J. Neural Transm. (Vienna) 130 (9) (2023) 1133–1151. [PubMed: 36786896]

[37]. Yoo JK, Badrov MB, Huang M, Bain RA, Dorn RP, Anderson EH, et al. , Abnormal sympathetic neural recruitment patterns and hemodynamic responses to cold pressor test in women with posttraumatic stress disorder, Am. J. Physiol. Heart Circ. Physiol. 318 (5) (2020) H1198–H1207. [PubMed: 32243771]

[38]. Tamaki S, Mano T, Sakata Y, Ohtani T, Takeda Y, Kamimura D, et al. , Interleukin-16 promotes cardiac fibrosis and myocardial stiffening in heart failure with preserved ejection fraction, PLoS One 8 (7) (2013) e68893. [PubMed: 23894370]

[39]. Zile MR, Baicu CF, Ikonomidis JS, Stroud RE, Nietert PJ, Bradshaw AD, et al. , Myocardial stiffness in patients with heart failure and a preserved ejection fraction: contributions of collagen and titin, Circulation 131 (14) (2015) 1247–1259. [PubMed: 25637629]

[40]. Lopez B, Gonzalez A, Hermida N, Valencia F, de Teresa E, Diez J, Role of lysyl oxidase in myocardial fibrosis: from basic science to clinical aspects, Am. J. Physiol. Heart Circ. Physiol. 299 (1) (2010) H1–H9. [PubMed: 20472764]

[41]. El Hajj EC, El Hajj MC, Ninh VK, Gardner JD, Inhibitor of lysyl oxidase improves cardiac function and the collagen/MMP profile in response to volume overload, Am. J. Physiol. Heart Circ. Physiol. 315 (3) (2018) H463–H473. [PubMed: 29775412]

[42]. Badenhorst D, Maseko M, Tsotetsi OJ, Naidoo A, Brooksbank R, Norton GR, et al. , Cross-linking influences the impact of quantitative changes in myocardial collagen on cardiac stiffness and remodelling in hypertension in rats, Cardiovasc. Res. 57 (3) (2003) 632–641. [PubMed: 12618225]

[43]. Kasner M, Westermann D, Lopez B, Gaub R, Escher F, Kuhl U, et al. , Diastolic tissue Doppler indexes correlate with the degree of collagen expression and cross-linking in heart failure and normal ejection fraction, J. Am. Coll. Cardiol. 57 (8) (2011) 977–985. [PubMed: 21329845]

[44]. Tual-Chalot S, Garcia-Collado M, Redgrave RE, Singh E, Davison B, Park C, et al. , Loss of endothelial Endoglin promotes high-output heart failure through peripheral arteriovenous shunting driven by VEGF signaling, Circ. Res. 126 (2) (2020) 243–257. [PubMed: 31805812]

[45]. Merino D, Villar AV, Garcia R, Tramullas M, Ruiz L, Ribas C, et al. , BMP-7 attenuates left ventricular remodelling under pressure overload and facilitates reverse remodelling and functional recovery, Cardiovasc. Res. 110 (3) (2016) 331–345. [PubMed: 27068510]

[46]. Swiercz AP, Iyer L, Yu Z, Edwards A, Prashant NM, Nguyen BN, et al. , Evaluation of an angiotensin type 1 receptor blocker on the reconsolidation of fear memory, Transl. Psychiatry 10 (1) (2020) 363. [PubMed: 33110066]

[47]. Moshfegh CM, Elkhatib SK, Watson GF, Drake J, Taylor ZN, Reed EC, et al. , S100a9 protects against the effects of repeated social defeat stress, Biol. Psychiatry Glob. Open Sci. 3 (4) (2023) 919–929. [PubMed: 37881565]

[48]. Bekhbat M, Drake J, Reed EC, Lauten TH, Natour T, Vladimirov VI, et al. , Repeated social defeat stress leads to immunometabolic shifts in innate immune cells of the spleen, Brain Behav. Immun. Health 34 (2023) 100690. [PubMed: 37791319]

[49]. Lerman YV, Lim K, Hyun YM, Falkner KL, Yang H, Pietropaoli AP, et al. , Sepsis lethality via exacerbated tissue infiltration and TLR-induced cytokine production by neutrophils is integrin alpha3beta1-dependent, Blood 124 (24) (2014) 3515–3523. [PubMed: 25278585]

[50]. Lin X, Sun Y, Yang S, Yu M, Pan L, Yang J, et al. , Omentin-1 modulates macrophage function via integrin receptors alphavbeta3 and alphavbeta5 and reverses plaque vulnerability in animal models of atherosclerosis, Front Cardiovasc Med 8 (2021) 757926. [PubMed: 34796216]

[51]. Barrett TJ, Corr EM, van Solingen C, Schlamp F, Brown EJ, Koelwyn GJ, et al. , Chronic stress primes innate immune responses in mice and humans, Cell Rep. 36 (10) (2021) 109595. [PubMed: 34496250]

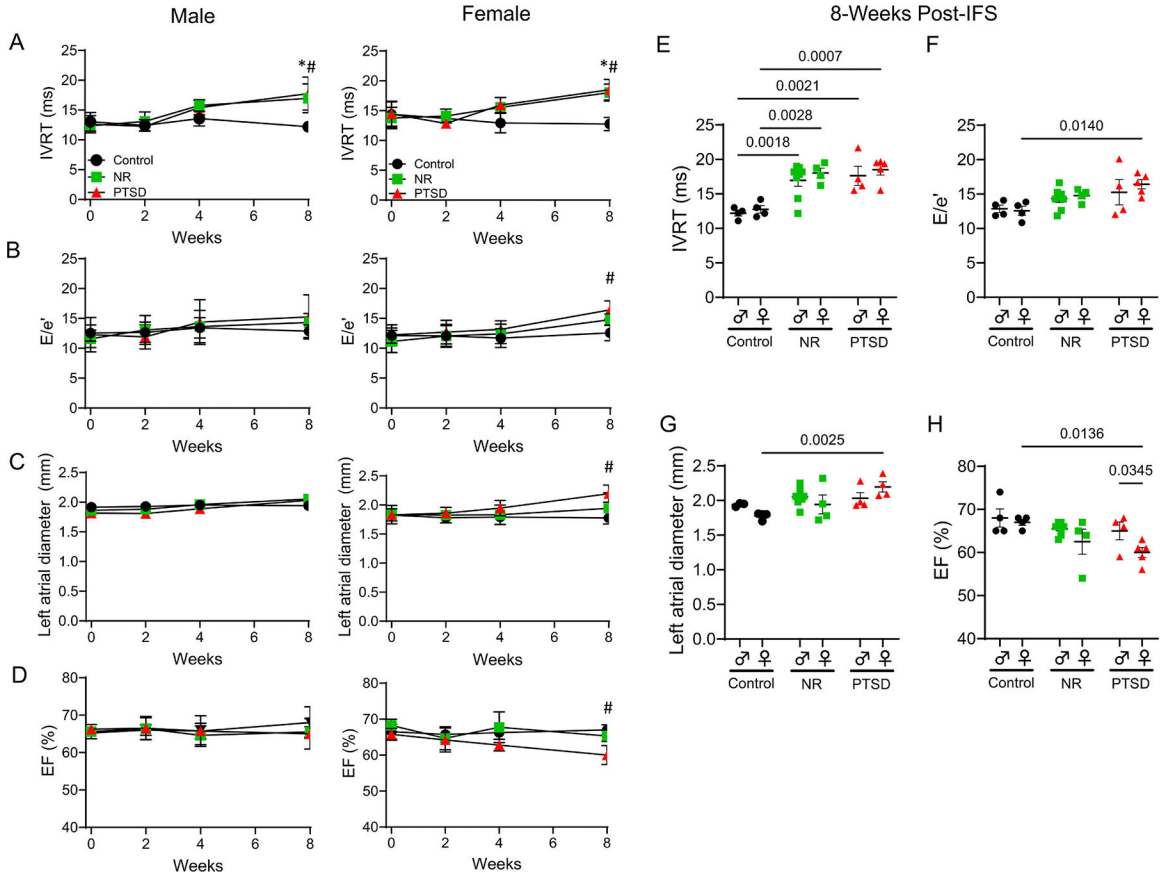

Fig. 1.

Female PTSD-like mice display diastolic dysfunction at 8-weeks post-IFS. A-D) Serial echocardiography and doppler measurements of male and female control, NR, and PTSD-like mice show male PTSD-like mice and NR mice of both sexes had a significant increase only in IVRT compared to controls while female PTSD-like mice had a significant increase in IVRT, E/e', and left atrial diameter and experienced a decrease in EF. *E*-H) Bar graphs of echocardiography data at 8-weeks post-IFS revealed clear differences between control and female PTSD-like mice. Female PTSD-like mice had decreased EF compared to male PTSD-like mice. Male control $n = 4$; Female control n = 4; Male NR n = 8; Female NR n = 4; Male PTSD-like $n = 4$; Female PTSD-like $n = 5$. Multiple group comparisons were analyzed by two-way ANOVA with Bonferroni posttest. #p < 0.05 vs Controls, *p < 0.05 vs NR; IVRT, isovolumetric relaxation time; EF, ejection fraction.

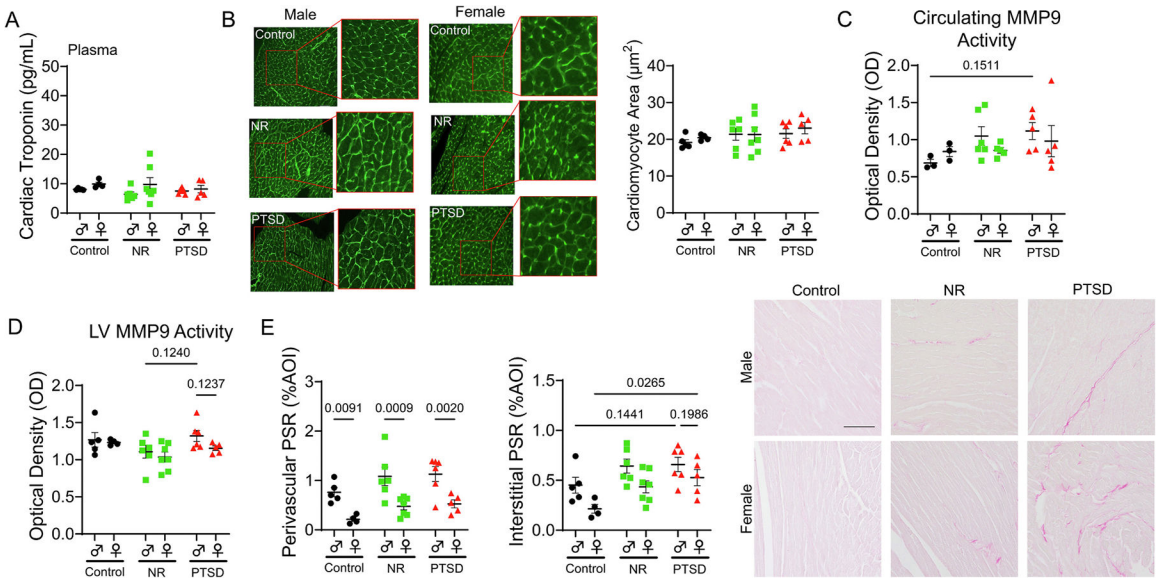

Fig. 2.

PTSD-like phenotype induced cardiac fibrosis in female mice at 4-weeks post-IFS. A) Circulating cardiac troponin was not increased between groups, indicating there is limited cardiomyocyte injury at 4-weeks. B) Wheat germ agglutinin stain revealed no differences in cardiomyocyte size in the left ventricle between groups at 4-weeks. C) Circulating matrix metalloproteinase (MMP)-9 activity at 4-weeks had an increased trend ($p = 0.1511$) in male PTSD-like mice compared to male controls. D) MMP-9 activity in the left ventricle was not significantly different between groups. E) Picrosirius red staining showed a sex difference in location of collagen volume fraction with male mice having higher levels of vascular collagen whereas, female PTSD-like mice had elevated interstitial collagen compared to sex-dependent controls. Multiple group comparisons were analyzed by two-way ANOVA with Bonferroni posttest. Sample size for panels A-B and D-E: Male control $n = 5$; Female control $n = 4$; Male NR $n = 6$; Female NR $n = 7$; Male PTSD-like n = 6; Female PTSD-like $n = 5$. Sample size for panel C: Male control $n = 3$; Female control n = 3; Male NR n = 6; Female NR n = 5; Male PTSD-like n = 5; Female PTSD-like n = 5. (For interpretation of the references to color in this figure legend, the reader is referred to the web version of this article.)

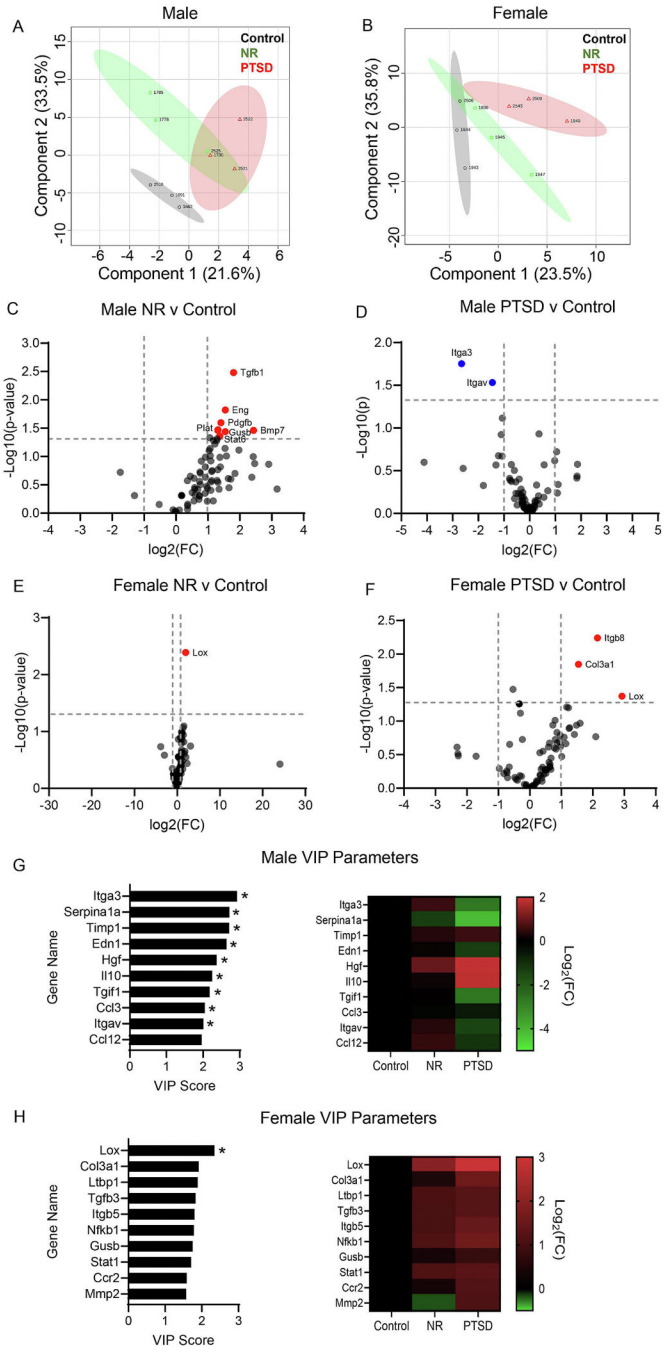

Fig. 3.

A) Male and B) female Partial Least-Squares Discriminant Analysis (PLSDA) plots show clear separation between groups based on genetic signatures collected from the left ventricle 4-weeks post-IFS. Volcano plots of C) male and D) female NR and PTSD-like mice indicate differently expressed genes with a fold change≥2.0 and a FDR > 0.05. G) Male and H) female Variance in Projection (VIP) scores along with the fold change of the corresponding gene indicate genes of interest that likely play a key role in pathology observed in the LV of PTSD-like mice. n = 3/sex/phenotype. PLSDA and VIP scores were calculated using

Metaboanalyst and a one-way ANOVA with Tukey's post hoc test to determine differentially expressed genes (defined as false discovery rate (FDR) adjusted $p < 0.05$). *indicates VIP score is >2; *Actb*, actin, beta; *Bmp7*, bone morphogenetic protein 7; *Col3a1*, collagen, type III, alpha 1; *Eng*, endoglin; *Gusb*, glucuronidase, beta; *Itga3*, integrin alpha 3; *Itgav*, integrin alpha V; Itgb8, integrin beta 8; *Lox*, lysyl oxidase; *Pdgfb*, platelet derived growth factor B polypeptide; *Plat*, plasminogen activator tissue; *Stat6*, signal transducer and activator of transcription 6; *Tgfb1*, transforming growth factor, beta 1.

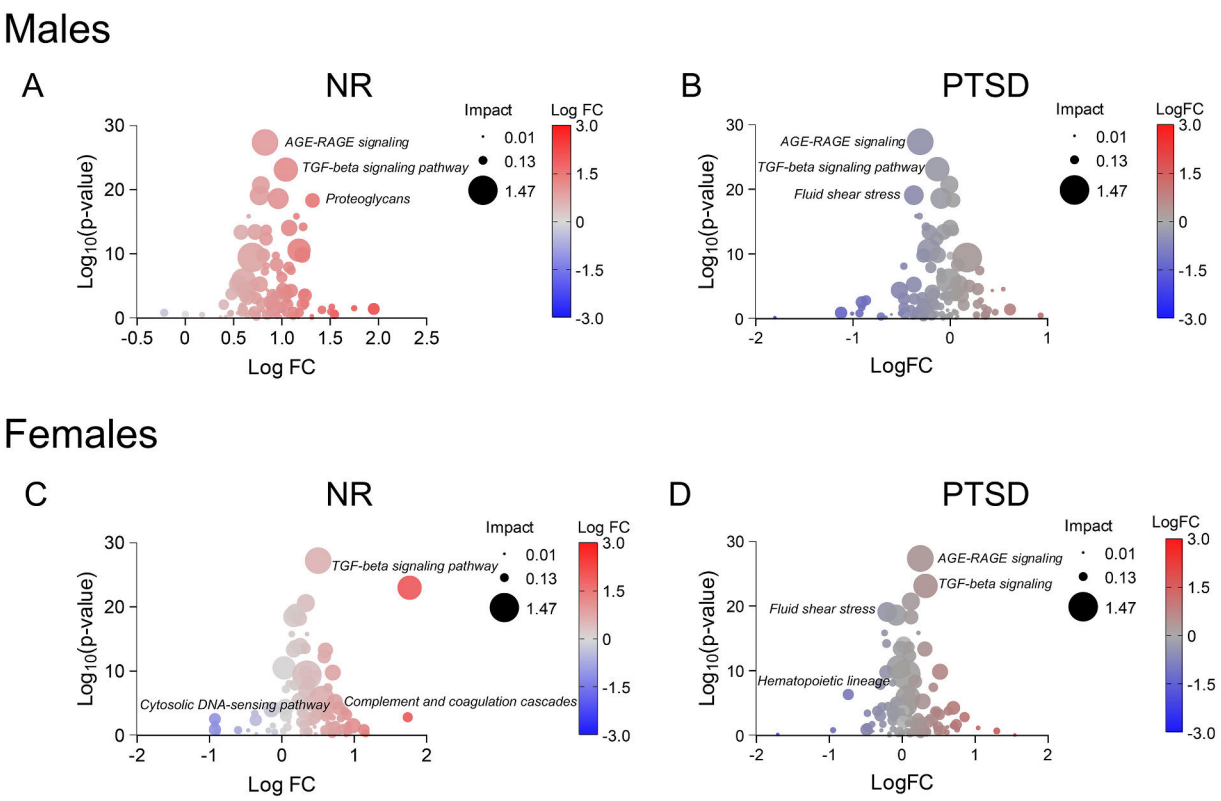

Fig. 4.

Bubble plot visualizes sex dependent activation of pathways enriched for male A) NR and B) PTSD-like mice and female C) NR and D) PTSD-like mice 4-weeks after IFS. n = 3/sex/phenotype. Pathway analysis was performed using Metaboanalyst. Fisher's exact test was used for pathway enrichment with degree centrality being used for topology measurement. Color of the bubble is based on average fold change of the genes within pathways. Size of bubble is dependent on number of genes identified within pathways.

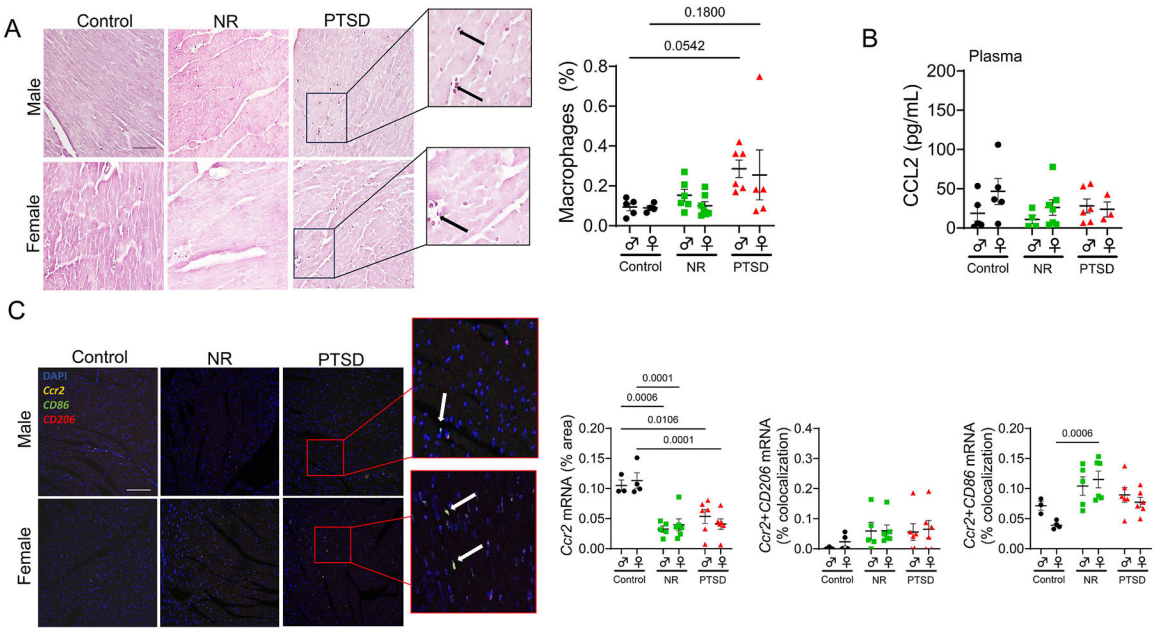

Fig. 5.

A) Male PTSD-like mice had an increased trend ($p = 0.0542$) in macrophages (Mac-3) in the left ventricle at 4-weeks post-IFS. No differences were observed in the female groups. Male control n = 3; Female control $n = 4$; Male NR $n = 6$; Female NR $n = 7$; Male PTSD-like n = 6; Female PTSD-like $n = 5$. B) No differences between phenotypes at 4-weeks post-IFS were observed in circulating levels of CCL2. Male control n = 4; Female control n = 4; Male NR n = 3; Female NR n = 6; Male PTSD-like n = 6; Female PTSD-like $n = 4$. C) Male and female NR and PTSD-like mice had decreased percent area of *Ccr2* mRNA expression compared to respective controls. No significant changes were seen in the amounts of *Ccr2* + *CD206* mRNA colocalization but female NR mice had an increase in *Ccr2* + *CD86* mRNA colocalization compared to female controls at 4-weeks post-IFS. Male control n = 3; Female control n = 4; Male NR n = 5; Female NR n = 7; Male PTSD-like n = 6; Female PTSD-like n = 5. Multiple group comparisons were analyzed by two-way ANOVA with Bonferroni posttest.

Table 1

Behavioral tests selected to mimic categories of the Diagnostic and Statistical Manual of Mental Disorders, Fifth Edition (DSM-5).

Symptom Cluster	Behavioral Assessment	Parameters in composite score
A-Trauma	Inescapable foot shock	• NA
B-Intrusiveness	Trauma-specific freezing in response to cue	• Activity after tone • Session fear extinction learning
C-Avoidance	Social Interaction Test	• Duration near new subject, no subject, center chamber • Total distance moved during trial
	Runway Enrichment	• Run duration • Velocity during run • # of runs away from enrichment source
D-Negative cognition/mood	Sucrose test	• Percentage of sucrose drank
	Novel Object Recognition	• Frequency near novel object, familiar object frequency, empty quadrants
E-Hyperarousal	Open Field Arena w/tone	• Cumulative duration in different zones • Cumulative duration in corners • Velocity 30 s after tone
F-Duration	≥1 month	• NA

Table 2

Clinical echocardiographic parameters in control and IFS male and female mice at 8-weeks post-IFS.

Phenotype	**Control**		**NR**		**PTSD-like**	
Sex	**Male (n = 4)**	**Female (n = 4)**	**Male (n = 8)**	**Female (n = 4)**	**Male (n = 4)**	**Female (n = 5)**
Heart rate (BPM)	453 ± 18	424 ± 7	459 ± 19	484 ± 15	445 ± 15	436 ± 11
EDV (uL)	59 ± 2	54 ± 4	58 ± 1	56 ± 1	60 ± 2	50 ± 2 *
ESV (uL)	19 ± 1	18 ± 1	20 ± 1	21 ± 2	21 ± 1	21 ± 1
EF (%)	68 ± 2	67 ± 1	66 ± 1	63 ± 2	65 ± 1	59 ± 1 *#
LAD (mm)	1.94 ± 0.02	1.78 ± 0.03	2.03 ± 0.05	1.93 ± 0.11	2.07 ± 0.06	2.19 ± 0.10 *
IVRT (ms)	13.67 ± 0.23	12.76 ± 0.55	16.58 ± 1.12	18.29 ± 0.61 *	17.81 ± 0.89 *	18.31 ± 0.97 *
E/e’	12.87 ± 0.53	12.57 ± 0.66	14.21 ± 0.72	14.71 ± 0.38	15.06 ± 1.18	16.93 ± 0.58 *
PATET	0.34 ± 0.03	0.34 ± 0.02	0.33 ± 0.04	0.40 ± 0.02	0.36 ± 0.03	0.40 ± 0.04

Values are presented as means±SEM; multiple group comparisons were analyzed by two-way ANOVA with Bonferroni test. EDV, end diastolic volume; ESV, end systolic volume; EF, ejection fraction; LAD, left atrial diameter; IVRT, isovolumetric relaxation time; PATET, pulmonary acceleration time/ejection time.

* $p < 0.05$ vs sex-specific controls

# $p < 0.05$ vs male PTSD-like.

Table 3

Behavioral parameters associated with intrusiveness and avoidance correlated with interstitial fibrosis primarily in female mice.

Behavior parameter		NR Male n=6	NR Female n=7	PTSD Male n=6	PTSD Female n=5
Intrusiveness score					
Session extinction coefficient	R^2	0.0725	0.3189	0.5738	***0.8080***
	p-value	0.6060	0.1866	0.0811	***0.0380***
Activity after tone 3	R^2	0.1776	0.0156	<0.0001	0.0130
	p-value	0.4053	0.7899	0.9866	0.8553
Activity after tone 4	R^2	0.0560	0.2354	0.1625	0.2663
	p-value	0.6516	0.2698	0.4281	0.3734
Activity after tone 5	R^2	0.0641	0.1386	0.0992	0.2922
	p-value	0.6283	0.4108	0.5432	0.3469
Avoidance score					
Duration in interaction zone with novel mouse	R^2	0.1666	0.0049	0.1394	0.1774
	p-value	0.4217	0.8820	0.4661	0.4801
Duration in empty chamber	R^2	0.3148	0.1571	0.3888	0.3356
	p-value	0.2467	0.3786	0.1859	0.3060
Duration in center chamber	R^2	0.0175	0.2322	0.0063	0.2070
	p-value	0.8026	0.2736	0.8814	0.4413
Total distance moved (social arena)	R^2	0.3119	0.1405	0.1441	0.0427
	p-value	0.2494	0.4075	0.4625	0.7389
Velocity across lighted runway	R^2	0.0565	0.2127	0.0284	0.2420
	p-value	0.6502	0.2976	0.7496	0.4000
Duration of enrichment runway test	R^2	0.0039	***0.5742***	0.0082	0.1965
	p-value	0.9066	***0.0485***	0.8648	0.4547
Frequency of runs away from enrichment	R^2	0.0404	0	0.0379	0.0932
	p-value	0.7026	0.9999	0.7119	0.6174
Negative mood/Cognition					
Sucrose Intake	R^2	0.1128	0	0.3218	0.0709
	p-value	0.5152	0.9999	0.2495	0.6650

Behavior parameter		NR Male n=6	NR Female n=7	PTSD Male n=6	PTSD Female n=5
Frequency (Novel Object)	R^2	0.1192	0.0080	0.1525	0.3172
	p-value	0.5028	0.8491	0.4440	0.3229
Frequency (Familiar Object)	R^2	0.2965	0.0156	0.0291	0.4205
	p-value	0.2639	0.7898	0.7468	0.2365
Frequency (Empty Chambers)	R^2	0.0420	0.0281	0.0130	0.1833
	p-value	0.6970	0.7194	0.8294	0.4721
Hyperactivity					
Duration in Outer Corners	R^2	0.0294	0.0282	0.0019	0.2158
	p-value	0.7452	0.7188	0.9354	0.4205
Duration in Outer Zone (Zone 1)	R^2	0.0727	0.1168	0.3298	0.3313
	p-value	0.6054	0.4532	0.2333	0.3099
Duration in Middle Zone (Zone 2)	R^2	0.1834	0.0233	***0.7837***	0.0206
	p-value	0.3968	0.7438	***0.0190***	0.8180
Duration in Inner Zone (Zone 3)	R^2	0.2441	0.0031	0.0941	0.0028
	p-value	0.3191	0.9063	0.5544	0.9323
Velocity after Tone	R^2	0.3596	0.0015	0.6120	0.3127
	p-value	0.2083	0.9350	0.0659	0.3271

Color of cell in table is reflective of directionality whereby red= positive correlation and blue= negative correlation; Bolding indicates correlation is significant.

Table 4

Top differentially expressed genes in the left ventricle of each group ranked by FDR.

Gene name	FC	Log_2FC	FDR
Male PTSD-like vs Controls			
Itga3	0.16	−2.65	0.02
Itgav	0.37	−1.45	0.03
Male NR vs Controls			
Tgfb1	3.49	1.80	<0.01
Eng	2.91	1.54	0.02
Pdgfb	2.65	1.41	0.03
Plat	2.48	1.31	0.03
Actb	2.48	1.31	0.03
Bmp7	5.38	2.43	0.03
Gusb	2.92	1.54	0.04
Stat6	2.59	1.37	0.04
Female PTSD-like vs Controls			
Itgb8	4.43	2.15	<0.01
Col3a1	2.91	1.54	0.01
Lox	7.60	2.93	0.04
Female NR vs Controls			
Lox	3.96	1.99	<0.01

FC, Fold change; Genes: *Actb*, actin, beta; *Bmp7*, bone morphogenetic protein 7; *Col3a1*, collagen, type III, alpha 1; *Eng*, endoglin; *Gusb*, glucuronidase, beta; *Itga3*, integrin alpha 3; *Itgav*, integrin alpha V; Itgb8, integrin beta 8; *Lox*, lysyl oxidase; *Pdgfb*, platelet derived growth factor B polypeptide; *Plat*, plasminogen activator tissue; *Stat6*, signal transducer and activator of transcription 6; *Tgfb1*, transforming growth factor, beta 1.